Optical nonreciprocity in an asymmetric cavity containing two asymmetrically arranged atoms

Xiuwen Xia,[1,2] Xinqin Zhang,[1,*] Jingping Xu,[2,†] Haozhen Li,[3] and Yaping Yang[2]

[1]*Institute of Atomic and Molecular Physics and Functional Materials, School of Mathematics and Physics, Jinggangshan University, Ji'an, Jiangxi 343009, People's Republic of China*

[2]*MOE Key Laboratory of Advanced Micro-Structure Materials, School of Physics Science and Engineering, Tongji University, Shanghai 200092, People's Republic of China*

[3]*College of Communication Engineering, Hangzhou Dianzi University, Hangzhou 310018, People's Republic of China*

(Received 22 August 2023; revised 1 February 2024; accepted 29 April 2024; published 13 May 2024)

We present a work of promoted optical nonreciprocity (ONR) in an asymmetrical cavity containing two asymmetrically arranged two-level atoms with a weak atom-atom interaction. The input-output relation is worked out by using a perturbative approach. Results show that the bistable-monostable-bistable phase transition would exist when the second atom is present, where the optical bistability and nonreciprocity change considerably. Contributions of two types of spatial asymmetries suggest that the ONR originates from the cooperation of the cavity spatial symmetry breaking and the optical nonlinearity, regardless of the atomic spatial symmetry breaking. In addition to the experimentally proved bistable ONR, a type of monostable ONR is proposed, which operates in the monostable phase. Both the ONR optimal regime and the block rate are boosted by adding the other atom in the cavity. Our findings suggest a prospective approach to the generation of a giant ONR by two atoms with unequal atom-cavity coupling strengths.

DOI: 10.1103/PhysRevA.109.053709

I. INTRODUCTION

The concept of optical nonreciprocity (ONR) is essential in optical diodes to generate a nonreciprocal transmission in the optical regime [1–5]. Optical diodes (ODs) are important to improve the optical stability by isolating a laser from reflection. The isolation of light is fundamental in information processing [6,7]. Up to now, several schemes have been implemented to break the transmission reciprocity, including collision-induced broadband ONR [8], magneto-optical isolators [9–11], nonlinear structures [12–15], time-dependent structures [16–18], optomechanical and circulating structures [19,20], quantum squeezing systems [21], and so on. However, most of these schemes are still too complicated, inefficient, active, and not all-optical.

Recently, a passive and all-optical ONR has been proposed in a single-atom-cavity coupling system [22]. Thereafter, a few-photon and high contrast OD has been successfully performed in the laboratory within an atom-cavity coupling system [23]. These studies pave the way to realize a highly efficient, passive and all-optical ONR within the simplest atom-cavity hybrid system. The saturation of atomic absorption produces a giant optical nonlinearity [24], and an asymmetrical cavity assembled with different walls breaks the spatial symmetry. Nonlinearities, spatial symmetry breakings, and immanent time-reversal symmetry breakings caused by the spontaneous decay of atoms, are essential to break optical reciprocity [25].

In this work, we modify the single-atom OD model by replacing a single two-level atom (TLA) with two weakly interacting TLAs, which unequally couple to the cavity mode. In the promoted OD model, two kinds of spatial symmetry breakings are present. The first one is the cavity asymmetry portrayed by the difference of cavity-loss rates of cavity walls, and the second one is the atomic asymmetry depicted by the imparity of two atom-cavity coupling strengths. Such a model without an atom-atom interaction has been introduced to improve the nonreciprocal unconventional photon blockade (NUCPB), showing that the cavity spatial asymmetry, in cooperation with the nonlinearity is the origin of NUCPBs, while the the asymmetrical arrangement of atoms can promote the NUCPBs into a wider operating regime [26].

The primary motivation of this work is to illustrate the contribution of the two types of spatial symmetry breakings to the ONR effect. As the atomic symmetry breaking provides an approach to manipulate optical nonreciprocity, another motivation in this work is to show how to improve the ONR effect by adding another atom.

II. THEORETICAL MODEL

The quantum model contains two weakly interacting TLAs with a transition frequency ω_a and a single-mode asymmetrical cavity with a frequency ω_c. The cavity is driven by a continuous-wave (cw) coherent field with a frequency ω_L as the input field. The schematic diagram is shown in Fig. 1. Two kinds of spatial symmetry breakings, i.e., the cavity asymmetry and the atomic asymmetry, are present in this model.

Cavity asymmetry is portrayed by the difference of cavity-loss rates. We define κ_1 and κ_2 as the cavity-loss rates of

*Corresponding author: jgsuzxq@163.com
†Corresponding author: xx_jj_pp@hotmail.com

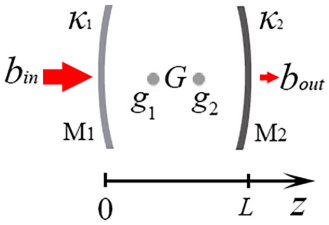

FIG. 1. Scheme of unequal double-TLA-cavity coupling system driven by a cw on the left wall M_1. Here, cavity-loss rate κ_1 (κ_2) represents the decay of the cavity mode through M_1 (M_2), and G is the atom-atom interacting strength. The gray circles in the cavity represent two TLAs with different atom-cavity coupling strengths g_1 and g_2.

cavity walls M_1 and M_2, fulfilling $\kappa_i = -c \ln R_i/2L$ $(i = 1, 2)$, where c is the velocity of light, R_i is the reflectivity of cavity wall M_i, and L is the effective length of the optical cavity. A cavity is symmetrical only in the case of $\kappa_1 = \kappa_2$. We present $\kappa_{\rm av} = (\kappa_1 + \kappa_2)/2$ as the average cavity-loss rate, and the total cavity-loss rate is $\kappa = \kappa_{\rm av} + \kappa_{\rm loss}$ where $\kappa_{\rm loss}$ represents the cavity mode dissipation. We fix $\kappa_{\rm loss}/\kappa \ll 1$ as the high-quality and low dissipation cavity discussed in this work.

Note that the intracavity field is very near to the perfect standing wave as the presence of high-quality cavity. We define the forward incident direction as the case of an external light incoming on the left wall (M_1) and outgoing through the right wall (M_2). Meanwhile, the backward case is the opposite with light propagating from M_2 to M_1. In order to examine the inequality between the counterpropagating intracavity waves, we separate the forward propagating field with amplitude a_f from the backward one with amplitude a_b, and denote a dimensionless factor $D = (|a_f| - |a_b|)/\max(|a_f|, |a_b|)$ as the inequality. Since $R_i \approx 1$, we rewrite $R_i = 1 - T_i$, where T_i is the near-zero transmission of cavity wall M_i. Taking the forward incident case as an example, the inequality of intracavity counterpropagating waves, $D = 1-\sqrt{R_2} \approx T_2/2$, is near zero as a high-quality cavity requires $T_i \approx 10^{-5}$ [23]. The near-zero inequality factor has no origins in the asymmetrical cavity. Any cavity, no matter its symmetry, without perfect walls ($R_i \neq 1$) faces the same puzzle. Therefore, the standing-wave approximation in a high-quality cavity is reasonable, in which the intracavity field can be treated as a standing wave by ignoring the mild difference of the near-zero node.

Atomic asymmetry is depicted by the imparity of atom-cavity coupling strengths. Following the standing-wave approximation, we denote $g_i = g \cos \phi_i (i = 1, 2)$ as the position-dependent atom-cavity coupling strength where g is the maximal atom-cavity coupling strength of a single atom. Here, $\phi_i = 2\pi z_i/\lambda_i$ relates to the position of atom z_i and the wavelength of the cavity mode $\lambda_c = 2\pi/\omega_c$. Atom arrangement is symmetric (or antisymmetric) only when $\phi_1 = \phi_2$ (or $\phi_1 = \phi_2 + \pi$), but it is arranged asymmetrically in common cases. We declare γ_a as the atom spontaneous decay rate and γ_n as the atom dephasing decay rate. Thus, the total atom decay rate is $\gamma = \gamma_a + \gamma_n$. We fix $\gamma_n = 0$ as cold atoms are considered in this work.

Furthermore, time-reversal symmetry breaking is present due to the spontaneous atom decay of atoms. Therefore, we present two kinds of spatial symmetry breakings: a giant optical nonlinearity and a time-reversal symmetry breaking in the atom-cavity coupling model, which are essential to produce the ONR effect.

In a frame rotating with the frequency of input field ω_L, the Hamiltonian of the hybrid system is

$$H/\hbar = \delta_a \sum_{i=1}^{2} \sigma_i^\dagger \sigma_i + \delta_c a^\dagger a + \sum_{i=1}^{2} g_i(\sigma_i^\dagger a + a^\dagger \sigma_i) + G(\sigma_1^\dagger \sigma_2 + \sigma_2^\dagger \sigma_1) + H_d. \quad (1)$$

The first two items are the energies of bare atoms and the cavity field. $\delta_a = \omega_a - \omega_L (\delta_c = \omega_c - \omega_L)$ represents the real detuning between the atom (cavity mode) and light. a is the annihilation operator of the cavity mode and $\sigma_m = |g\rangle_{m\ m}\langle e|$ $(m = 1, 2)$ is the atomic pseudospin operators. The third and the fourth items represent the atom-cavity coupling and atom-atom interaction respectively. The weak atom-atom interaction is described by dipole-dipole coupling $G = \frac{\mu^2}{4\pi\varepsilon_0 r^3}(1 - 3\cos^2\theta)$, where $\boldsymbol{\mu}$ is the electric dipole moment, $\boldsymbol{r}$ is the displacement between two atoms, and θ is the angle between the two vectors. The last item presents the cavity driving as $H_d = \eta(a + a^\dagger)$, where η is the effective driving strength. Note that the effective driving strength $\eta = \sqrt{\kappa_m} b_{\rm in}$ ($m = 1$ or 2) relies on the incident direction. Here, $b_{\rm in} = \sqrt{n_{\rm in}}$ and $n_{\rm in} = P_{\rm in}/\hbar\omega_L$ characterize the normalized amplitude and the intensity of the incoming field with power $P_{\rm in}$, respectively. We focus on the ONR property in the forward case at first, and that in the backward case can be obtained by alternating κ_1 with κ_2, g_1 with g_2, and G with its conjugate G^*.

Heisenberg equations dominate the dynamic relations of all operators. Following previous works [22,24,27], we adopt the semiclassical approximation where the quantum correlations between atomic operators and field operators can be neglected. This approximation is applicable in the weak-coupling regime and for most of the strong-coupling regime, but it is not valid in the ultrastrong-coupling regime. By introducing the scaled mean-field theory and omitting the fluctuation variables of operators, we get the Heisenberg-Langevin equations, reading

$$\dot{s}_m = -i\Delta_a s_m - ig_m(-2s_{z,m})\alpha - iG(-2s_{z,m})s_n, \quad (2)$$

$$\dot{s}_{z,m} = -ig_m s_m^* \alpha + ig_m \alpha^* s_m - iGs_m^* s_n + iGs_n^* s_m - \gamma_a(s_{z,m} + 1/2), \quad (3)$$

$$\dot{\alpha} = -i\Delta_c \alpha - i(g_1 s_1 + g_2 s_2) - i\eta. \quad (4)$$

Here, we denote these mean values, i.e., $s_m = \langle\sigma_m\rangle$, $s_{z,m} = \langle\sigma_{z,m}\rangle$, and $\alpha = \langle a\rangle$, to represent the operators' expectations, where $\sigma_{z,m} = (\sigma_m^\dagger \sigma_m - \sigma_m \sigma_m^\dagger)/2$ and $m \neq n = 1$ or 2. We represent $\Delta_a = \delta_a - i\gamma/2$ and $\Delta_c = \delta_c - i\kappa/2$ as the complex detunings.

The optical input-output relation is solved by using a perturbative approach. We neglect the transient process as an ONR occurs in the steady state. Since the interaction between atoms is weak, we set $G = 0$ to get the zeroth-order solutions, and the influence of weak G is treated as a first-order perturbation. From Eqs. (2)–(4), we get the zeroth-order stationary

solution of s_m, reading

$$s_m^{(0)} = \frac{2g_m s_{z,m}^{(0)}\alpha}{\Delta_a}. \tag{5}$$

A cavity field should emerge from both mirrors to form the reflected light and transmission light. By introducing the quantum input-output theory [22], the output field amplitude from M_2 is $b_{\rm out} = -i\sqrt{\kappa_2}a$, which leads the relation between the cavity and output field to $n_t = \kappa_2 n_c$. Here, we represent $n_c = \langle a^\dagger a\rangle$ as the cavity photon number. And $n_{\rm in} = \langle b_{\rm in}^\dagger b_{\rm in}\rangle$ and $n_t = \langle b_{\rm out}^\dagger b_{\rm out}\rangle$ are the average incoming and the transmitting photons per unit time, respectively.

Injecting Eq. (5) into the evolution equation for $s_{z,m}$, we obtain the zeroth-order stationary solution for $s_{z,m}$, reading

$$s_{z,m}^{(0)} = -\frac{1}{2}\frac{1}{1+y_m}, \tag{6}$$

where y_m is the saturation parameters related to the saturation of atoms in the cavity and can be written as

$$y_m = n_t/P_{{\rm crit},m}, \tag{7}$$

where $P_{{\rm crit},m}(m = 1, 2)$ is the critical power in the cavity necessary to reach $s_{z,m} = -1/4$, satisfying

$$P_{{\rm crit},m} = \frac{\kappa_2\gamma_a\left(\delta_a^2+\gamma_h^2\right)}{4g_m^2\gamma_h}. \tag{8}$$

Here, we rewrite the half decay as $\gamma_h = \gamma/2$. In the case of $\gamma_n = 0$, the critical power can be simplified as $P_{{\rm crit},m} = \kappa_2(\delta_a^2+\gamma_h^2)/2g_m^2$.

Now we consider the influence of the weak interatomic coupling. The evolution of s_m shows that the steady solution consists of zeroth- and first-order components, written as

$$s_m = s_m^{(0)} + s_m^{(1)}, \tag{9}$$

where the first-order item is

$$s_m^{(1)} = \frac{2Gs_{z,m}^{(0)}s_n^{(0)}}{\Delta_a}. \tag{10}$$

Injecting Eqs. (9) and (10) into the evolution equation for α, we can obtain the stationary solution that recovers the relation between $n_{\rm in}$ and n_t, reading

$$n_{\rm in} = n_t\left(f_c^2+f_d^2\right)\big/\kappa_1\kappa_2, \tag{11}$$

where $f_c = \kappa + f_1\gamma_h + f_2\gamma_h - 2f_1f_2\gamma\delta_a G/g_1g_2$ and $f_d = \delta_c - f_1\delta_a - f_2\delta_a - 2f_1f_2(\gamma_h^2-\delta_a^2)G/g_1g_2$, and $f_m = g_m^2/(\delta_a^2+\gamma_h^2)(1+y_m)$ $(m = 1, 2)$ is a nonlinear dimensionless factor of atom m. Factor f_m degenerates into a linear one by setting $y_m = 0$ when the incident light is too weak to saturate the atoms. Also, $f_m = 0$ when atom m is absent ($g_m = 0$). The first items in f_c and f_d are contributions of the cavity. The second and third items in them are contributions of atom 1 and atom 2, respectively. The last items in them represent the contributions of the atom-atom coupling. As we focus on the weak atom-atom interaction limitation ($G \ll g$) in the Purcell regime ($\gamma < g < \kappa$), the contributions of weak interatomic coupling are high-order smaller than the contributions of the atoms and cavity.

Thus, we get the input-output relation in the forward incident case. By injecting f_m and y_m into the input-output relation and after some rearrangements, we can get a quintic equation of n_t, i.e., $P^{(5)}(n_t) = 0$, in which the polynomial coefficients are related to the input power $n_{\rm in}$. If we drive the system with a given power $n_{\rm in}$, it may experience a multistable procedure when the quantic equation has five positive roots, or it may experience a bistable procedure when the equation has three positive roots, otherwise it may experience a monostable procedure when the equation has only one positive root. In this work, we focus our discussion on the bistable and monostable optical experiences.

For the backward incident case, one can get a similar input-output equation only by interchanging g_1 and κ_1 with g_2 and κ_2 as we take coupling strengths as real. By analyzing the input-output relations in detail, we get the following conclusions theoretically. First, the ONR does not appear in symmetrical cavity systems, regardless of atomic symmetry breakings. The transposition of two unequal atoms does not correlate with the optical bistability (OB) and ONR as g_1 and g_2 appear in pairs. Therefore, it is not possible to manipulate the ONR by interchanging sites between atoms. Similar to the origination of the NUCPB in an asymmetric cavity [26], the ONR originates from the cavity asymmetry rather than the atomic asymmetry. Second, once the OB occurs in a certain cavity with fixed κ and $\kappa_{\rm loss}$, bistability always occurs no matter how the cavity symmetry breakings are. This conclusion is consistent with the result of a single-atom OB [22]. This suggests that we can discuss the threshold condition of the OB effect in the symmetrical cavity, while the cavity asymmetries only play the role of enhancing or suppressing the OB regime.

The atom-atom coupling causes a push-and-pull effect of energy levels [28], which disturbs the optical input-output relation. Here, we present a magic detuning to avoid the influence of weak atom-atom coupling. By letting the last item in f_c be zero and $f_d = 0$, we get the magic detuning condition, fulfilling $\delta_a = 0$ and $\delta_c = 2f_1f_2\gamma_h^2 G/g_1g_2$.

III. IMPROVEMENT OF OPTICAL NONRECIPROCITY

Since the optical nonlinearity and the feedback are inherent in this model, the OB effect has been proposed in a single-atom case, and observed in the few-atom and atomic gas cases [22,23,29,30]. As an OB occurs regardless of cavity asymmetries, we focus on the symmetric cavity case to discuss the condition to produce the OB effect.

Here, we normalize all of the couplings and damping rates by taking $g_{\rm at} \equiv 1$, ignore the atom dephasing decay and the cavity nonradiation decay by setting $\gamma_n = \kappa_{\rm loss} = 0$, and focus on the resonant case by setting $\delta_a = \delta_c = 0$. We plot Fig. 2(a) to show a typical OB in the resonant case with symmetric boundaries. Two critical input intensities n_l and n_u identifying the boundaries of the bistable regime are plotted to separate the linear ($n_{\rm in} < n_l$) and the saturated regimes ($n_{\rm in} > n_u$) from the bistable regime.

As shown in Fig. 2(a), the bistable regimes are marked by the gray rectangles, which are bordered by the threshold intensities n_l and n_u. Light is almost blocked in the linear regime. The anharmonicity, induced by the energy level splitting of the dressed states, suppresses light transmission. In the saturated regime, light is almost transparent. The saturation of

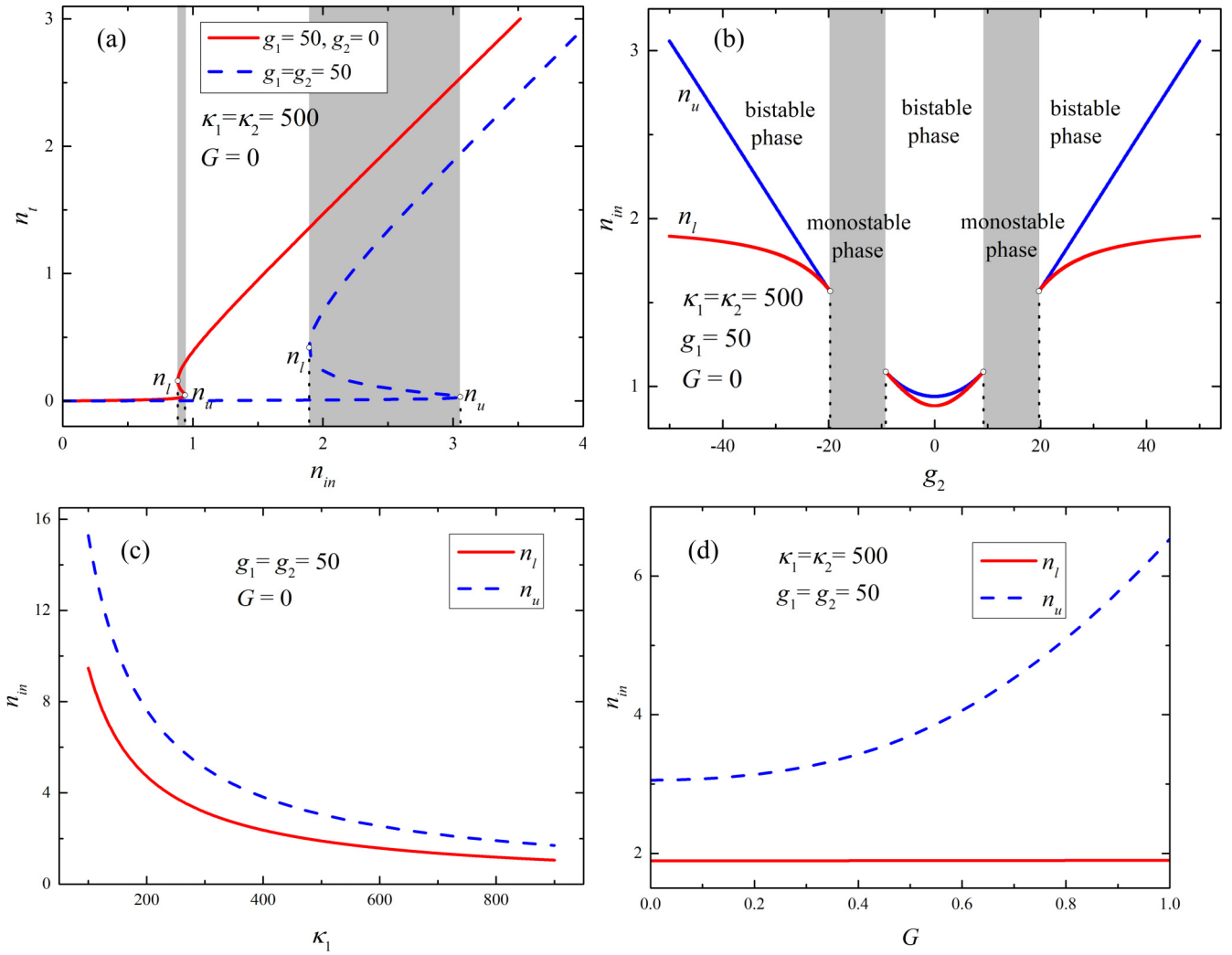

FIG. 2. OB in an atom-cavity coupling system. We take $\gamma_{at} = 1$, $\delta_a = \delta_c = \gamma_n = \kappa_{loss} = 0$, $\kappa_{av} = 500$ for convenience. (a) Single-atom OB ($g_1 = 50$ and $g_2 = 0$, dashed blue line) and double-atom OB ($g_1 = g_2 = 50$, solid red line) in the symmetric cavity. The bistable regimes are marked by the gray rectangles, which are bordered by the threshold intensities (black dotted lines) n_l and n_u. (b) Phase transition in the symmetric cavity with two atoms. The monostable phases are presented by the gray rectangles while the other areas belong to the bistable phases. (c) Cavity asymmetry enhanced OB ($\kappa_1 < \kappa_2$) and suppressed bistability ($\kappa_1 > \kappa_2$) in the asymmetric cavity. (d) Weak dipole-dipole interaction enhanced OB in the symmetrical cavity. In both panels (c) and (d), the lower critical intensity n_l is shown by the solid red line, and the upper critical intensity n_u is shown by the dashed blue line.

atoms prevents atoms from further light-matter interactions, which leads light to propagate through the atom-cavity system easily like through an empty cavity. In the bistable regime, the trajectory of light, whether it follows the upper branch or the lower branch, is contingent upon its driving history. OB critical intensities n_l and n_u, as well as the OB regime $|n_u - n_l|$, are enlarged as two identical atoms.

In order to show the influence of unequal atoms to the OB effect, we plot the critical intensities (n_l and n_u) in a symmetrical cavity by fixing $g_1 = 50$ and shifting g_2 from -50 to 50, as shown in Fig. 2(b). As the OB regimes do not vary when we change the sign of g_2, we focus our discussion on the case of $g_2 > 0$. With increasing g_2 from 0 to 9.2, the OB critical intensities n_l and n_u increase while OB regimes $|n_u - n_l|$ decrease and vanish, which indicates a phase transition from the bistable phase to a monostable phase. However, the OB manner reappears when $g_2 > 19.7$. Such bistable-monostable-bistable phase transitions in the atom-cavity coupling system are not discovered in the single-atom-cavity coupling system [22]. Therefore, we can separate the monostable phase from the bistable phases, as shown in Fig. 2(b). The monostable phases are marked by the gray rectangles while the other areas belong to the bistable phases. The existence of monostable phases indicates that we can realize a kind of giant ONR in the monostable phases with two unequal atoms.

The double-atom OB is controllable by adjusting the cavity symmetry breakings. We take the forward incident case as an example and plot OB critical intensities as functions of symmetry breaking in Fig. 2(c). Both the OB critical intensities and the OB regimes decrease with the increasing of κ_1. A promoted OB effect is present in the asymmetrical cavity of $\kappa_1 < \kappa_2$ and a suppressed OB effect appears in the asymmetric cavity of $\kappa_1 > \kappa_2$. The result is consistent with that of a single-atom OB [22].

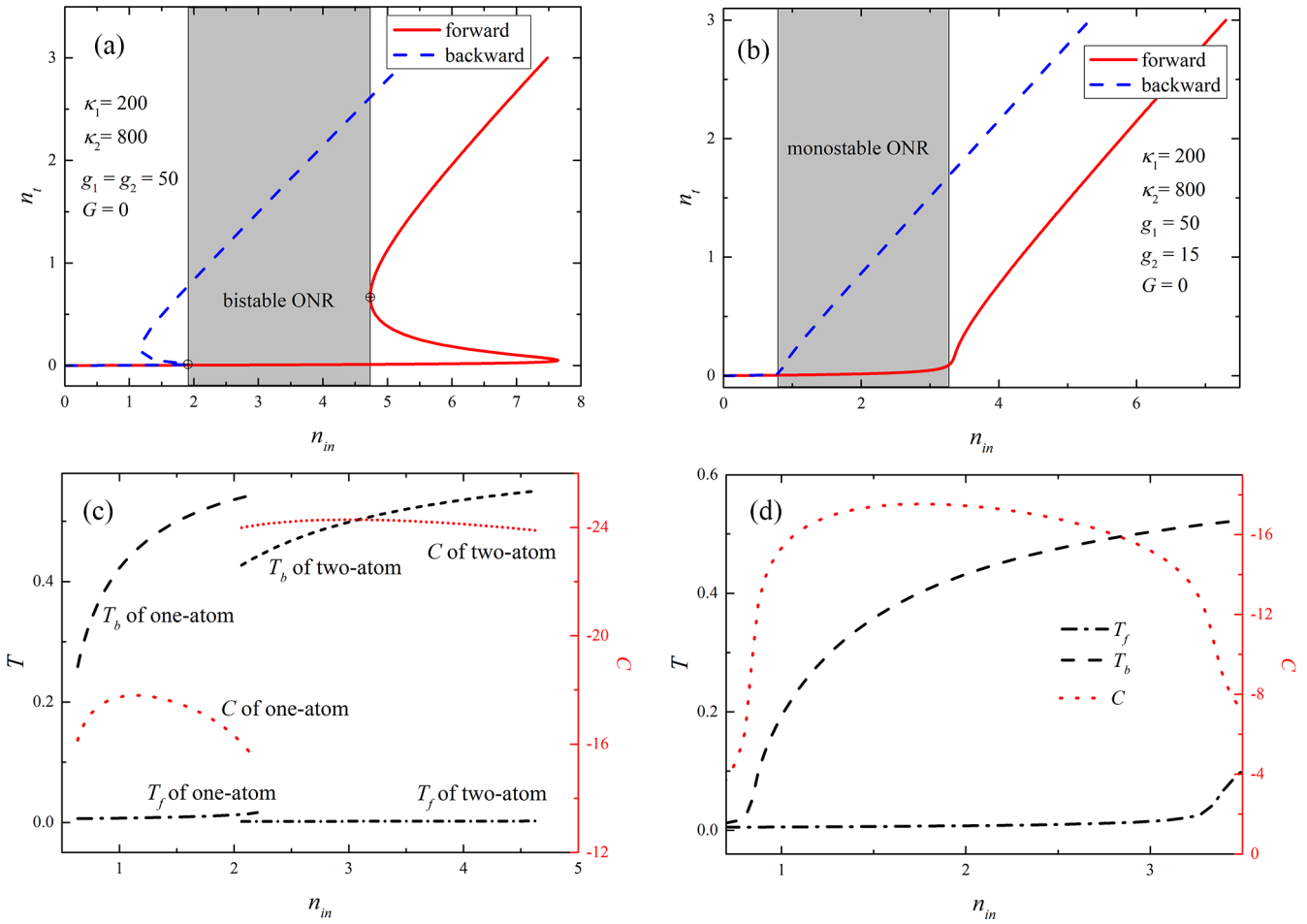

FIG. 3. ONR in the bistable phase (a) and in the monostable phase (b). We take $\gamma_{at} = 1$, $\delta_a = \delta_c = \gamma_n = \kappa_{loss} = 0$, $\kappa_{av} = 500$, and $G = 0$ for convenience. For the bistable ONR, $g_1 = g_2 = 50$, and the optimal ONR regime is between $n_{u-backward}$ of the backward case and $n_{l-forward}$ of the forward case, which is marked by the gray rectangle. For the monostable ONR, $g_1 = 50$ and $g_2 = 15$, and the optimal ONR regime is marked by the gray rectangle. Panel (c) shows the bistable ONR transmission coefficients T_f and T_b and the block contrast C for both the single-atom case ($g_1 = 50$ and $g_2 = 0$) and the double-atom case ($g_1 = g_2 = 50$). Panel (d) shows the monostable ONR properties for double-atom case ($g_1 = 50$ and $g_2 = 15$).

The weak atom-atom interaction is beneficial to generate OB, as shown in Fig. 2(d). With the increase of weak interatomic coupling, both the OB critical intensities and the OB regime increase a lot. Furthermore, with the increase of G, n_l increases very slightly while n_u increases greatly. This indicates that one can manipulate the upper critical intensity n_u by the weak dipole-dipole interaction.

Now we examine the ONR property in the bistable and the monostable phases. We make the asymmetrical cavity as $\kappa_1 = 200$ and $\kappa_2 = 800$, and calculate the input-output function in both forward and backward incident cases, as shown in Figs. 3(a) and 3(b). In the bistable phase, output light undergoes a typical bistable manner. This shows that the bistable ONR is conspicuous since OB threshold intensities are associated with light incident directions. The critical intensity $n_{l-forward}$ (n_l in the forward case) separates far away from the critical intensity $n_{u-backward}$ (n_u in the backward case). The bistable ONR optimal regime is denoted by $|n_{l-forward} - n_{u-backward}|$ and is marked by the gray rectangle in Fig. 3(a). In the ONR optimal regime, light is blocked in the forward case while it is transparent in the backward case.

In the monostable phase, it needs a larger input power to saturate atoms in the forward case, whereas a lower power in the backward case, which leads to the production of the monostable ONR, as shown in Fig. 3(b). The monostable ONR optimal regime is marked by the gray rectangle. Light wil be blocked in the forward case whereas it will be transparent in the backward case. Therefore, both the bistable and monostable ONRs are present in this work.

In order to examine the quality of this kind of optical diode with an asymmetrical atom-cavity structure, we introduce the transmission coefficient of $T = n_t/n_{in}$, and rewrite it as T_f and T_b to represent T in the forward and the backward incident cases. And, we define optical contrast $C = 10 \times |\log_{10}(T_f/T_b)|$ as the diode block rate. We plot T_f, T_b, and C in the bistable ONR optimal regime, as shown in Fig. 3(c). In the optimal window of the double-atom case ($g_1 = g_2 = 50$), the giant bistable ONR occurs whose block rate is around -24 dB (short dotted red line), while in the optimal window of the single-atom case ($g_1 = 50$ and $g_2 = 0$), the bistable ONR is around -17 dB (dotted red line). Comparing the single-atom and the two-atom cases, the ONR optimal regime is enlarged

from 1.6237 to 2.8252 and the block rate C is promoted from around -17 to -24 dB. The ONR effect is improving a lot when two atoms are involved.

The monostable ONR only occurs in the double-atom case, as shown in Fig. 3(d). It does not block light as efficiently as the double-atom bistable ONR, but the block rate is comparable to that of the single-atom bistable ONR. In the optimal window, the monostable ONR occurs whose block rate is around -16 dB (dotted red line), and the ONR optimal regime is enlarged a lot compared to the single-atom bistable ONR.

As a result, we declare that the monostable and bistable solutions of the Heisenberg-Langevin equations are stable. As we only care about the stationary solution of the system in the Purcell regime ($\gamma < g < \kappa$), any deviation induced by initial conditions will disappear when $t \to \infty$. We estimate the Lyapunov spectrum by using the standard method [31]. Firstly, we calculate the dynamic of Lyapunov exponents by setting the initial conditions as two ground atoms and a zero cavity photon. In the monostable regime, we take parameters $\kappa = 500$, $\delta_a = \delta_c = G = 0$, $g_1 = 50$, $g_2 = 15$, and $n_{\text{in}} = 1.5$ as an example, and the maximum of the Lyapunov exponents is $\lambda_{\max} = -0.51$. In the bistable regime we take parameters $\kappa = 500$, $\delta_a = \delta_c = G = 0$, $g_1 = g_2 = 50$, and $n_{\text{in}} = 2.5$ as an example. The maximum exponent is $\lambda_{\max} = -0.48$. Then, we change the initial conditions and perform the calculation again. As expected, all of the Lyapunov exponents are less than zero even when we change the initial conditions greatly. This indicates that the evolution of the Heisenberg-Langevin equations in the Purcell regime is stable.

IV. CONCLUSION

In summary, we present a simple-structured OD model containing two weakly interacting TLAs unequally coupled to an asymmetric cavity, where cavity spatial symmetry and atomic spatial symmetry breakings are involved. By using the quantum perturbation method, we analytically obtain the input-output relation. The optical properties do not change much with the weak atom-atom interaction, while the OB and the OD behaviors change considerably when the second atom is present. We examine the contribution of two specific asymmetries to the ONR and show that the ONR originates from the cooperation of cavity spatial symmetry breaking and optical nonlinearity, while atomic spatial symmetry breaking can promote or suppress the ONR. Although it is not possible to manipulate the ONR by exchanging interatomic sites, we can manipulate the OB and ONR by tuning the coupling strength of the second atom. In addition to the bistable ONR, we find the monostable ONR.

ACKNOWLEDGMENTS

This work is supported by the National Natural Science Foundation of China (Grants No. 12164022, No. 11864018, and No. 12174288), Natural Science Foundation of Jiangxi Province of China (20232BAB201044), Scientific Research Foundation of the Education Department of Jiangxi Province of China (Grant No. GJJ211039), and China Postdoctoral Science Foundation (2023M732028).

[1] D.-W. Wang, H.-T. Zhou, M.-J. Guo, J.-X. Zhang, J. Evers, and S.-Y. Zhu, Phys. Rev. Lett. **110**, 093901 (2013).
[2] L. Fan, J. Wang, L. T. Varghese, H. Shen, B. Niu, Y. Xuan, A. M. Weiner, and M. Qi, Science **335**, 447 (2012).
[3] X. Hu, Z. Li, J. Zhang, H. Yang, Q. Gong, and X. Zhang, Adv. Funct. Mater. **21**, 1803 (2011).
[4] C. Wang, X.-L. Zhong, and Z.-Y. Li, Sci. Rep. **2**, 674 (2012).
[5] B. Megyeri, G. Harvie, A. Lampis, and J. Goldwin, Phys. Rev. Lett. **121**, 163603 (2018).
[6] L. J. Aplet and J. W. Carson, Appl. Optics **3**, 544 (1964).
[7] Y. Zhang, L. Shi, C. T. Chan, K. H. Fung, and K. Chang, Phys. Rev. Lett. **130**, 203801 (2023).
[8] C. Liang, B. Liu, A.-N. Xu, X. Wen, C. Lu, K. Xia, M. K. Tey, Y.-C. Liu, and L. You, Phys. Rev. Lett. **125**, 123901 (2020).
[9] R. L. Espinola, T. Izuhara, M.-C. Tsai, J. R. M. Osgood, and H. Dötsch, Opt. Lett. **29**, 941 (2004).
[10] T. R. Zaman, X. Guo, and R. J. Ram, Appl. Phys. Lett. **90**, 023514 (2007).
[11] L. Bi, J. Hu, P. Jiang, D. H. Kim, G. F. Dionne, L. C. Kimerling, and C. A. Ross, Nat. Photonics **5**, 758 (2011).
[12] K. Gallo, G. Assanto, K. R. Parameswaran, and M. M. Fejer, Appl. Phys. Lett. **79**, 314 (2001).
[13] D. Roy, Phys. Rev. A **96**, 033838 (2017).
[14] S. R. K. Rodriguez, V. Goblot, N. C. Zambon, A. Amo, and J. Bloch, Phys. Rev. A **99**, 013851 (2019).
[15] A. Muñoz de las Heras, R. Franchi, S. Biasi, M. Ghulinyan, L. Pavesi, and I. Carusotto, Phys. Rev. Appl. **15**, 054044 (2021).
[16] Z. Yu and S. Fan, Nat. Photonics **3**, 91 (2009).
[17] M. Kang, A. Butsch, and P. S. J. Russell, Nat. Photonics **5**, 549 (2011).
[18] F. Song, Z. Wang, E. Li, B. Yu, and Z. Huang, Phys. Rev. Appl. **18**, 024027 (2022).
[19] M.-A. Miri, F. Ruesink, E. Verhagen, and A. Alù, Phys. Rev. Appl. **7**, 064014 (2017).
[20] B. He, L. Yang, X. Jiang, and M. Xiao, Phys. Rev. Lett. **120**, 203904 (2018).
[21] L. Tang, J. Tang, M. Chen, F. Nori, M. Xiao, and K. Xia, Phys. Rev. Lett. **128**, 083604 (2022).
[22] X. Xia, J. Xu, and Y. Yang, Phys. Rev. A **90**, 043857 (2014).
[23] P. Yang *et al.*, Phys. Rev. Lett. **123**, 233604 (2019).
[24] A. Auffèves-Garnier, C. Simon, J.-M. Gérard, and J.-P. Poizat, Phys. Rev. A **75**, 053823 (2007).
[25] D. Jalas *et al.*, Nat. Photonics **7**, 579 (2013).
[26] X. Xia, X. Zhang, J. Xu, H. Li, Z. Fu, and Y. Yang, Opt. Express **30**, 7907 (2022).
[27] C. W. Gardiner and M. J. Collett, Phys. Rev. A **31**, 3761 (1985).
[28] X. Zhang, X. Xia, J. Xu, H. Li, Z. Fu, and Y. Yang, Chin. Phys. B **31**, 074204 (2022).
[29] A. Szoke, V. Daneu, J. Goldhar, and N. Kurnit, Appl. Phys. Lett. **15**, 376 (1969).
[30] H. Gibbs, S. McCall, and T. Venkatesan, Phys. Rev. Lett. **36**, 1135 (1976).
[31] K. Ramasubramanian and M. S. Sriram, Phys. D (Amsterdam, Neth.) **139**, 72 (2000).